JARO 17: 609–619 (2016)
DOI: 10.1007/s10162-016-0582-8

JARO
Journal of the Association for Research in Otolaryngology

Research Article

Symmetric Electrode Spanning Narrows the Excitation Patterns of Partial Tripolar Stimuli in Cochlear Implants

Xin Luo[1,3] and Ching-Chih Wu[1,2]

[1]*Department of Speech, Language, and Hearing Sciences, Purdue University, 715 Clinic Dr., West Lafayette, IN 47907, USA*
[2]*School of Electrical and Computer Engineering, Purdue University, 465 Northwestern Av., West Lafayette, IN 47907, USA*
[3]*Department of Speech and Hearing Science, Arizona State University, Coor Hall, 975 S. Myrtle Av., P.O. Box 870102, Tempe, AZ 85287, USA*

Received: 29 March 2016; Accepted: 10 August 2016; Online publication: 25 August 2016

ABSTRACT

In cochlear implants (CIs), standard partial tripolar (pTP) mode reduces current spread by returning a fraction of the current to two adjacent flanking electrodes within the cochlea. Symmetric electrode spanning (i.e., separating both the apical and basal return electrodes from the main electrode by one electrode) has been shown to increase the pitch of pTP stimuli, when the ratio of intracochlear return current was fixed. To explain the pitch increase caused by symmetric spanning in pTP mode, this study measured the electrical potentials of both standard and symmetrically spanned pTP stimuli on a main electrode EL8 in five CI ears using electrical field imaging (EFI). In addition, the spatial profiles of evoked compound action potentials (ECAP) and the psychophysical forward masking (PFM) patterns were also measured for both stimuli. The EFI, ECAP, and PFM patterns of a given stimulus differed in shape details, reflecting the different levels of auditory processing and different ratios of intracochlear return current across the measurement methods. Compared to the standard pTP stimuli, the symmetrically spanned pTP stimuli significantly reduced the areas under the curves of the normalized EFI and PFM patterns, without shifting the pattern peaks and centroids (both around EL8). The more focused excitation patterns with symmetric spanning may have caused the previously reported pitch increase, due to an interaction between pitch and timbre perception. Being able to reduce the spread of excitation, pTP mode symmetric spanning is a promising stimulation strategy that may further increase spectral resolution and frequency selectivity with CIs.

Keywords: cochlear implant, electrode spanning, current focusing, tripolar mode, spread of excitation, electrical field imaging, evoked compound action potential, forward masking pattern

INTRODUCTION

A major bottleneck of current cochlear implant (CI) technology is that the spectral resolution and frequency selectivity are too limited to support high-level performance for speech recognition in noise and music perception. Only 12–22 electrodes are implanted in the cochlea, and each of these electrodes is typically stimulated with the current returned to an extracochlear ground. Such monopolar (MP) stimulation generates a wide electrical potential field and subsequently a broad neural excitation pattern along the tonotopic axis of the cochlea. Two adjacent electrodes stimulated in MP mode may activate a common group of neurons and thus affect the perception of channel-specific information. The so-called channel interaction varies across electrodes and patients, depending on the survival of spiral ganglions and the placement of electrode array (see Bierer 2010 for a review).

Correspondence to: Xin Luo · Department of Speech and Hearing Science · Arizona State University · Coor Hall, 975 S. Myrtle Av., P.O. Box 870102, Tempe, AZ 85287, USA. Telephone: (480) 965-9251; email: xinluo@asu.edu

One way to increase frequency selectivity and reduce channel interaction is to use focused electrode configurations (e.g., Bierer 2007; Landsberger et al. 2012; Zhu et al. 2012), while other approaches attempt to place the electrode array close to the auditory neurons (Tykocinski et al. 2001; Middlebrooks and Snyder 2007). This study focused on a current focusing technique using the partial tripolar (pTP) stimulation mode. In pTP mode, each main electrode is stimulated with part of the current returned to two flanking intracochlear electrodes and the rest to the extracochlear ground. The proportion of current returned within the cochlea (i.e., the compensation coefficient σ) can be adjusted to find a tradeoff between current focusing and loudness growth. Both animal and human studies have shown that pTP mode with a compensation coefficient greater than 0.5 may produce narrower electrical fields and excitation patterns than MP mode (e.g., Mens and Berenstein 2005; Bierer et al. 2010; Goldwyn et al. 2010; Landsberger et al. 2012; Zhu et al. 2012). Compared to an MP-mode speech processing strategy, a pTP-mode speech processing strategy matched in the stimulation pulse rate and the number of channels significantly improved speech recognition in noise, most likely due to reduced channel interactions (Srinivasan et al. 2013).

Recently, Wu and Luo (2014) reported electrode spanning (i.e., returning current to non-adjacent basal and/or apical flanking electrodes) to generate additional distinctive pitches, increase the number of channels, and handle defective electrodes in pTP mode. For example, compared to standard $pTP_{(7,8,9)}$ (with EL7 as the apical return electrode, EL8 as the main electrode, and EL9 as the basal return electrode), apically spanned $pTP_{(6,8,9)}$ (with EL6 instead of EL7 as the apical return electrode) was higher in pitch, while basally spanned $pTP_{(7,8,10)}$ (with EL10 instead of EL9 as the basal return electrode) was lower in pitch (see Fig. 4 in Wu and Luo 2014). A computational model suggested that apical spanning greatly reduced the current spread on the apical side (but not on the basal side) and thus pushed the excitation centroid (or center of gravity) basally for a higher pitch. The exact excitation pattern mirrored around the main electrode was predicted for basal spanning by the simple computational model (Wu and Luo 2014).

Interestingly, symmetrically spanned $pTP_{(6,8,10)}$ (with EL6 and EL10 as the non-adjacent apical and basal return electrodes) was higher in pitch than standard $pTP_{(7,8,9)}$ for five out of six CI ears (see Fig. 11 in Wu and Luo 2014). Note that the two tested stimuli had the same stimulation rate, compensation coefficient (ranging from 0.6 to 0.8), and loudness. The pitch difference between $pTP_{(6,8,10)}$ and $pTP_{(7,8,9)}$ was difficult to explain using the computational model, because the modeled effects of symmetric spanning were symmetric on both sides of the excitation pattern so that the excitation centroid of $pTP_{(6,8,10)}$ was predicted to be the same as that of $pTP_{(7,8,9)}$ (both on EL8). In other words, the symmetric changes to the two edges of the excitation pattern with $pTP_{(6,8,10)}$ would not predict a consistent pitch increase relative to $pTP_{(7,8,9)}$.

Wu and Luo (2014) offered two possible explanations for the higher pitch of $pTP_{(6,8,10)}$ than that of $pTP_{(7,8,9)}$. The first hypothesis was based on the pitch-ranking results of apical and basal spanning alone. It was found that relative to standard $pTP_{(7,8,9)}$, the pitch increase caused by apical spanning [i.e., $pTP_{(6,8,9)}$] was more salient than the pitch decrease caused by basal spanning [i.e., $pTP_{(7,8,10)}$]. The favored current flow from the apex to the base with CIs (e.g., Jolly et al. 1996; Vanpoucke et al. 2004b) was not considered in the computational model but may make the reduction of current spread with apical spanning more effective than that with basal spanning in real CIs. Consequently, when both apical and basal spanning were used in $pTP_{(6,8,10)}$, the two edges of the excitation pattern may not have the model-predicted symmetric changes. Instead, the reduction of current spread on the apical side may be greater than that on the basal side so that the excitation centroid may shift basally to elicit a higher pitch than $pTP_{(7,8,9)}$.

The second hypothesis was based on the possible interaction between pitch and timbre. With a fixed main electrode, more focused stimuli tend to be higher in pitch than less focused stimuli (Litvak et al. 2007; Wu and Luo 2014). For example, Wu and Luo (2014) found that pitch increased when the compensation coefficient of pTP stimuli (and presumably, the degree of current focusing) increased. It is possible that the purer/cleaner sound quality and the greater pitch strength of more focused stimuli may be confounded with a pitch increase (Landsberger et al. 2012). The higher pitch of $pTP_{(6,8,10)}$ than that of $pTP_{(7,8,9)}$ may also be due to the same reason, since the modeling results of Wu and Luo (2014) suggested that $pTP_{(6,8,10)}$ may have an overall more focused excitation pattern (despite a slightly broader excitation near the peak) than $pTP_{(7,8,9)}$.

In summary, symmetric spanning in pTP mode represents a very interesting case for the study of pitch perception mechanisms with CIs. As in Wu and Luo (2016), the intracochlear electrode voltages as well as physiological and psychophysical excitation patterns of $pTP_{(7,8,9)}$ and $pTP_{(6,8,10)}$ were measured and compared in this study. In specific, electrical field imaging (EFI) records intrascalar potentials and relies

on the assumption of uniform neural distribution along the cochlea. Electrically evoked compound action potentials (ECAP) give information on neural activity that is not available in electrical field imaging. Finally, psychophysical forward masking (PFM) has both peripheral and central contributions. The different measurement methods were used to reveal the effects of symmetric spanning at different stages along the auditory pathway and test the two hypotheses from Wu and Luo (2014). At issue was whether $pTP_{(6,8,10)}$ had a more basally located excitation centroid or an overall more focused excitation pattern than $pTP_{(7,8,9)}$. Therefore, features such as the peak, centroid, and area under the curve were extracted from each pattern and analyzed as a function of stimulation mode and measurement method. The results may not only shed light on the pitch perception mechanisms with CIs but also suggest novel stimulation modes that may improve spectral resolution with CIs.

METHODS

Subjects

The same subjects from Wu and Luo (2016) participated in this study. All four CI subjects were female, postlingually deafened, and implanted with the Advanced Bionics HiFocus 1J electrode array. The subjects were also tested in Wu and Luo (2014). Subjects S1, S2, S3, and S4 in this study were subjects S1, S2, S3, and S5 in Wu and Luo (2014), respectively. Subject S4 in Wu and Luo (2014) was not tested in this study, because her neural survival was poor due to the removal of NF2 tumors, and she did not consistently perceive the pitch increase with symmetric spanning in pTP mode. Subject S3 was tested in both ears (S3L and S3R, respectively). Table 1 lists the subject demographic details. All subjects gave informed consent and were compensated for their participation. This study was approved by the Purdue IRB committee.

Stimuli and Procedure

The EFI, ECAP, and PFM patterns of standard $pTP_{(7,8,9)}$ and symmetrically spanned $pTP_{(6,8,10)}$ were measured using the same methods as in Wu and Luo (2016). The stimuli and procedure for each measurement are briefly described here, and more details can be found in Wu and Luo (2016).

The Electrical Field Imaging and Modeling software (v 1.4, Advanced Bionics, Antwerp, Belgium) was used to measure the EFI patterns. Sine waves of 2.5 ms and 3000 Hz were presented at a sub-threshold level of 32 μA in the two tested pTP modes. The compensation coefficients were identical to those in the pitch-ranking test (Wu and Luo 2014), as listed in Table 1. The compensation coefficient of each subject had the highest value that allowed for full loudness growth within the compliance limit of the implant system. The electrical potentials on the non-stimulated electrodes were directly recorded, while those on the stimulated electrodes (e.g., EL6, EL8, and EL10 for $pTP_{(6,8,10)}$) were estimated by linearly adding the electrical potentials recorded from the corresponding MP stimulation of each stimulated electrode with the relevant current weighting. For each MP stimulation, such as the one on EL8, the electrical potential on the stimulated electrode was estimated by fitting the potentials on the apical non-stimulated electrodes with an exponential curve (e.g., Vanpoucke et al. 2004a; Berenstein et al. 2010), fitting those on the basal non-stimulated electrodes with another exponential curve and averaging the extrapolated potentials of the two curves on the stimulated electrode. Using this method, good agreement has been found between the recorded and estimated potentials on the non-stimulated electrodes of pTP stimuli (Berenstein et al. 2010; Wu and Luo 2016).

The Bionic Ear Data Collection System (v 1.17, Advanced Bionics, Sylmar, CA) was used to record the ECAP responses, and the stimulus artifacts were removed using the forward masking subtraction method (Abbas et al. 1999). The spread of neural excitation for $pTP_{(7,8,9)}$ and $pTP_{(6,8,10)}$ was measured as the change in ECAP amplitude with different locations of the MP-mode maskers along the electrode array. ECAP amplitudes recorded from EL6 and EL10 were averaged to derive the final ECAP patterns of $pTP_{(7,8,9)}$. For $pTP_{(6,8,10)}$, the two ECAP recording electrodes were EL7 and EL9. The probe and masker stimuli were biphasic pulses with a shorter phase duration (32 μs) and a lower pulse rate (20 Hz) than those in the pitch-ranking test of Wu and Luo (2014), which were 226 μs and 1000 Hz, respectively. The changes were necessary for the ECAP recording to avoid prolonged stimulus artifacts and strong neural adaptation. The compensation coefficients of the pTP-mode probes were also reduced (see Table 1) so that equal loudness at the soft but comfortable levels could be reached. Unfortunately, the most comfortable levels of the pTP-mode probes exceeded the compliance limit of the implant system even with the reduced compensation coefficients and were thus not used for ECAP recording. The poor loudness growth of pTP-mode probes motivated us to use MP-mode maskers at the most comfortable levels. Although the MP-mode maskers had broad excitation patterns that may limit the chance of observing a difference between the probe patterns, the sufficient loudness of the MP-mode maskers may facilitate the

TABLE 1
Demographic details, pitch-ranking results, equal-loudness most comfortable levels, and tested compensation coefficients of individual subjects

Subject	*Age*	*Etiology*	*Years with prosthesis*	*Percentage that $pTP_{(6,8,10)}$ was judged as higher in pitch than $pTP_{(7,8,9)}$*	*Equal-loudness most comfortable levels in microampere for $pTP_{(6,8,10)}$ and $pTP_{(7,8,9)}$*	*σ used for pitch ranking, EFI and PFM measurements*	*σ used for ECAP recording*
S1	85	Sudden hearing loss	5	100	365, 384	0.60	0.55
S2	45	Meningitis	9	90	303, 423	0.80	0.50
S3L	67	Hereditary deafness	3	95	302, 358	0.75	0.40
S3R	67	Hereditary deafness	8	90	372, 350	0.65	0.55
S4	64	Unknown	5	100	236, 250	0.60	0.60

masking of the pTP-mode probes, which was critical for the success of the forward masking subtraction method. Note that pitch ranking was not tested for the pTP-mode probes in ECAP recording. Therefore, the measured ECAP patterns may not directly explain the pitch-ranking results of Wu and Luo (2014) but may reveal how the distributions of neural excitation are affected by electrode spanning in pTP mode with smaller σ values and lower loudness levels.

The PFM patterns of $pTP_{(7,8,9)}$ and $pTP_{(6,8,10)}$ were also measured using the Bionic Ear Data Collection System. A three-interval forced choice, two-down/one-up adaptive procedure was used to measure the unmasked and masked thresholds of 20-ms probes along the electrode array in standard pTP mode (with a compensation coefficient of 0.65 for subject S1 and 0.75 for the other subjects). The 300-ms maskers $pTP_{(7,8,9)}$ and $pTP_{(6,8,10)}$ stopped 10 ms before the probe onset. Both maskers and probes were 1000-Hz biphasic pulse trains with a 226-μs phase duration. The maskers were the same stimuli as those in the pitch-ranking test with an equal loudness at the most comfortable level (Wu and Luo 2014). The compensation coefficients of the maskers are listed in Table 1. The elevations of probe thresholds induced by the maskers (i.e., the dB differences between masked and unmasked probe thresholds) were calculated as the PFM patterns of the maskers.

Data Analysis

Each EFI, ECAP, or PFM pattern was normalized to its peak amplitude. As in Wu and Luo (2016), the peak (i.e., the electrode location with the highest amplitude) and the centroid (i.e., the arithmetic mean location of all electrodes weighted by the amplitudes) were calculated for each pattern. Wu and Luo (2016) calculated the width of each pattern at 75 % of the peak amplitude to quantify the spread of excitation only around the main electrode. Instead, this study also considered the electrodes further away from the main electrode and calculated the whole area under the curve of each pattern to better describe the spread of excitation. To test the hypothesized pitch-change mechanisms of symmetric spanning in pTP mode, the peaks, centroids, and areas of $pTP_{(7,8,9)}$ and $pTP_{(6,8,10)}$ were compared by paired t tests or Wilcoxon signed-rank tests (when the normality test failed) for EFI, ECAP, and PFM patterns, respectively. Two-way repeated measures analyses of variance (RM ANOVAs) were then used to compare the peaks, centroids, and areas of $pTP_{(7,8,9)}$ and $pTP_{(6,8,10)}$ across EFI, ECAP, and PFM patterns. Holm-Sidak post hoc t tests were used for the two-way RM ANOVAs. Since normalizing the patterns only gave information on the slopes or widths of the patterns but not on the peak amplitudes, the original, non-normalized patterns were also presented.

RESULTS

The same subjects have also participated in the study of Wu and Luo (2014) to rank $pTP_{(7,8,9)}$ and $pTP_{(6,8,10)}$ in pitch. The pitch-ranking results from Wu and Luo (2014) showed that all subjects consistently judged $pTP_{(6,8,10)}$ as higher in pitch than $pTP_{(7,8,9)}$, with the percentage ranging from 90 to 100 % (see Table 1). Also, the equal-loudness most comfortable levels (MCLs) were not significantly different between $pTP_{(6,8,10)}$ and $pTP_{(7,8,9)}$ (paired t test $t_4 = 1.55$, $p = 0.19$). The following EFI, ECAP, and PFM patterns were measured for a better understanding of the pitch-ranking results.

EFI Patterns

Figure 1 shows the original (upper panels) and normalized EFI patterns (lower panels) as a function of recording electrode for $pTP_{(7,8,9)}$ (filled circles) and $pTP_{(6,8,10)}$ (open squares) in each subject. Different subjects had different non-normalized electrical potentials, due to their different conductivities of cochlear tissues and surface properties of electrodes. The EFI patterns of both $pTP_{(7,8,9)}$ and $pTP_{(6,8,10)}$ had a single sharp peak on EL8. The centroids of the roughly symmetric EFI patterns were also around EL8 (as indicated by the symbols near the x-axis) and not significantly different for $pTP_{(7,8,9)}$ and $pTP_{(6,8,10)}$ (Wilcoxon signed rank test $Z = 0.41$, $p = 0.81$). The non-normalized electrical potentials of $pTP_{(6,8,10)}$ were higher than those of $pTP_{(7,8,9)}$ on EL7, EL8, and EL9. Note that the electrical potentials on EL7 and EL9 were recorded for $pTP_{(6,8,10)}$ but estimated for $pTP_{(7,8,9)}$. Thus, the actual differences in electrical potentials between $pTP_{(6,8,10)}$ and $pTP_{(7,8,9)}$ on EL7 and EL9 may differ from those in Figure 1. In contrast, the original electrical potentials of $pTP_{(6,8,10)}$ were lower than those of $pTP_{(7,8,9)}$ on EL1–6 and EL10–16. The spread of excitation thus slightly increased around the excitation peak but greatly reduced outside of the excitation peak with symmetric spanning in pTP mode. Overall, the areas under the curves of the normalized EFI patterns for $pTP_{(6,8,10)}$ were significantly smaller (by 10–30 %) than those for $pTP_{(7,8,9)}$ ($t_4 = 9.03$, $p < 0.001$). A Pearson correlation analysis showed that the percentage reduction of the normalized EFI pattern area with symmetric spanning was significantly correlated with the pTP compensation coefficient ($r = 0.94$, $p = 0.02$). That is, the more current returned to the flanking electrodes, the more reduction of the normalized EFI pattern area caused by symmetric spanning.

ECAP Patterns

Figure 2 shows the original (upper panels) and normalized ECAP patterns (lower panels) as a function of masker electrode for $pTP_{(7,8,9)}$ (filled circles) and $pTP_{(6,8,10)}$ (open squares) in each subject. Subject S2 had higher non-normalized ECAP amplitudes than the other subjects had, possibly because she was younger and had longer duration of CI use. With symmetric spanning, the non-normalized ECAP amplitudes reduced on most of the electrodes for S1 and S3R but increased around EL8 for S2, S3L, and S4. Zero values and non-monotonic changes were observed in the ECAP amplitudes, possibly due to the low signal-to-noise ratios in ECAP measures of pTP stimuli. Thus, there was not a single prominent peak for some ECAP patterns, and the ECAP centroids did not shift in a consistent way with symmetric spanning in pTP mode. Paired t tests also did not reveal significant differences in the ECAP peaks ($t_4 = 0.54$, $p = 0.62$) and ECAP centroids (as indicated by the symbols near the x-axis; $t_4 = 1.48$, $p = 0.21$) between $pTP_{(7,8,9)}$ and $pTP_{(6,8,10)}$. The areas under the curves of the normalized ECAP patterns were largely similar for $pTP_{(7,8,9)}$ and $pTP_{(6,8,10)}$. One exception was that the ECAP patterns for S3L with symmetric spanning in pTP mode were truncated at both ends of the electrode array, because the neural responses were too weak to be measured in these cases. Overall, the effect of stimulation mode on the areas under the curves of the normalized ECAP patterns did not reach significance ($t_4 = 2.58$, $p = 0.06$). The limited reduction of the normalized ECAP pattern area with symmetric spanning was not significantly correlated with the small compensation coefficient of pTP stimuli ($r = 0.79$, $p = 0.11$).

PFM Patterns

Figure 3 shows the original (upper panels) and normalized threshold shifts (lower panels) of standard pTP probes induced by the forward maskers $pTP_{(7,8,9)}$ (filled circles) and $pTP_{(6,8,10)}$ (open squares) as a function of probe electrode in each subject. For S1 and S2, the non-normalized probe threshold shifts greatly reduced across the whole electrode array with symmetric spanning. However, for the other subjects, the non-normalized probe threshold shifts remained similar on EL8 and only reduced on some electrodes away from EL8 with symmetric spanning. The PFM patterns of both maskers generally showed a single peak on EL8 and decreased monotonically toward the apex and base when the masker moved away from the probe. No significant differences were found in the PFM peaks (Wilcoxon signed rank test $Z = 1.00$, $p = 1.00$) and PFM centroids (as indicated by the symbols near the x-axis; $t_4 = 0.67$, $p = 0.54$) between $pTP_{(7,8,9)}$ and $pTP_{(6,8,10)}$. The normalized PFM amounts of $pTP_{(6,8,10)}$ were smaller than or similar to those of $pTP_{(7,8,9)}$ both around and outside of the excitation peak. These observations differed from those in the normalized EFI patterns (see Fig. 1). The areas under the curves of the normalized PFM patterns were significantly smaller ($t_4 = 10.31$, $p < 0.001$) for $pTP_{(6,8,10)}$ than for $pTP_{(7,8,9)}$ (by 9–17 %). There was no significant correlation between the compensation coefficient of pTP stimuli and the percentage reduction of the normalized PFM

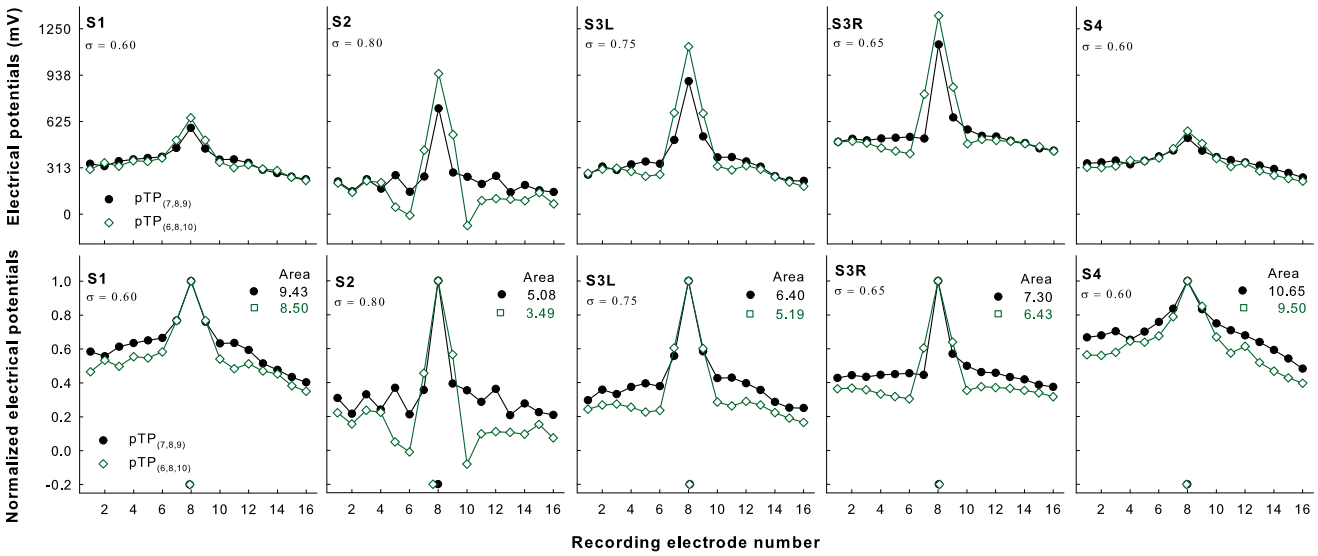

FIG. 1. Original (*upper panels*) and normalized EFI patterns (*lower panels*) as a function of recording electrode for $pTP_{(7,8,9)}$ (*filled circles*) and $pTP_{(6,8,10)}$ (*open squares*) in each subject (columns 1–5, respectively). The centroid of each pattern is indicated by the corresponding *symbol* near the x-axis. The area under the curve of each normalized pattern is shown at the *upper right corner*. The tested compensation coefficient for each subject is shown at the *upper left corner*.

pattern area with symmetric spanning ($r = 0.76$, $p = 0.14$).

Comparisons Across Measurement Methods

The peaks, centroids, and areas under the curves of the normalized EFI, ECAP, and PFM patterns for $pTP_{(7,8,9)}$ and $pTP_{(6,8,10)}$ are shown in Figure 4. The ECAP peaks were more variable across subjects and located more basally than the EFI and PFM peaks. However, a two-way RM ANOVA on the locations of the pattern peaks did not reveal significant effects of measurement method ($F_{2,\ 8} = 2.82$, $p = 0.12$), stimulation mode ($F_{1,\ 8} = 0.00$, $p = 1.00$), and their interaction ($F_{2,\ 8} = 0.55$, $p = 0.60$). The EFI and ECAP centroids were around the main electrode EL8, while the PFM centroids were located slightly more apically. Again, no significant effects were found for measurement

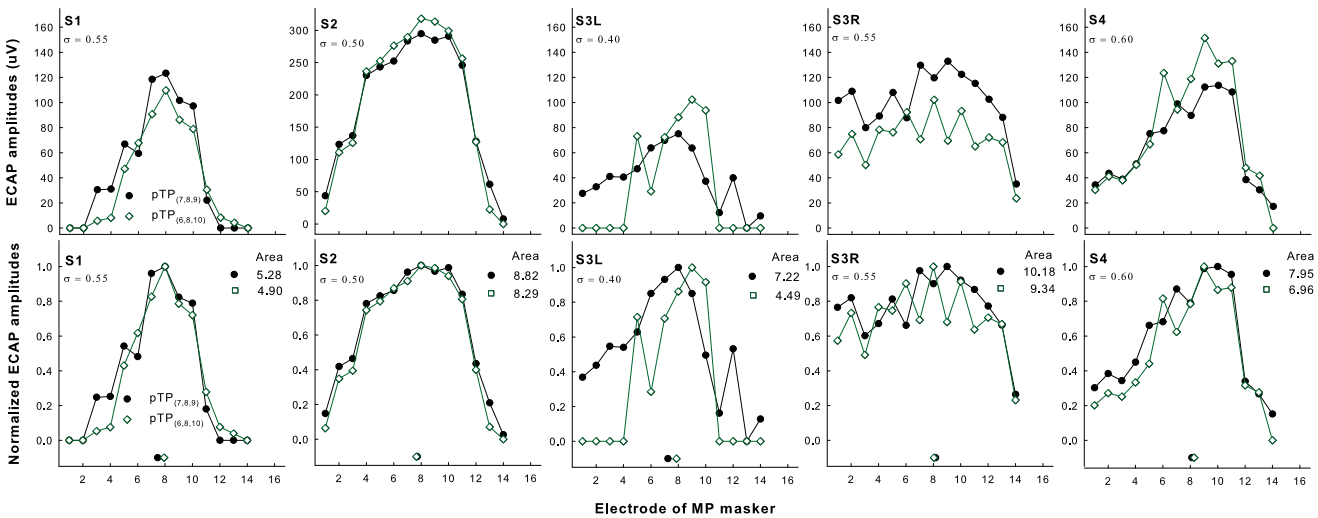

FIG. 2. Original (*upper panels*) and normalized ECAP patterns (*lower panels*) as a function of masker electrode for $pTP_{(7,8,9)}$ (*filled circles*) and $pTP_{(6,8,10)}$ (*open squares*) in each subject (columns 1–5, respectively). The centroid of each pattern is indicated by the corresponding *symbol* near the x-axis. The area under the curve of each normalized pattern is shown at the *upper right corner*. The tested compensation coefficient for each subject is shown at the *upper left corner*.

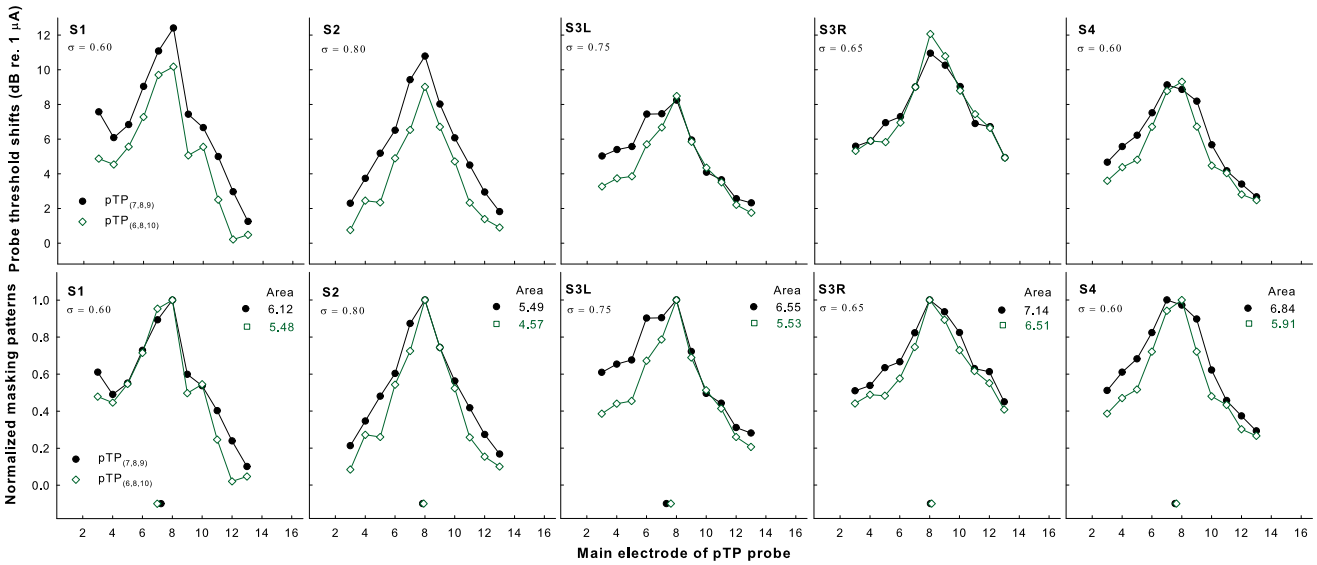

FIG. 3. Original (*upper panels*) and normalized PFM patterns (*lower panels*) as a function of probe electrode for $pTP_{(7,8,9)}$ (*filled circles*) and $pTP_{(6,8,10)}$ (*open squares*) in each subject (columns 1–5, respectively). The centroid of each pattern is indicated by the corresponding *symbol* near the x-axis. The area under the curve of each normalized pattern is shown at the *upper right corner*. The tested compensation coefficient for each subject is shown at the *upper left corner*.

method ($F_{2,\ 8} = 2.43$, $p = 0.15$), stimulation mode ($F_{1,\ 8} = 1.01$, $p = 0.37$), and their interaction ($F_{2,\ 8} = 2.02$, $p = 0.20$) on the locations of the pattern centroids.

The areas under the curves of the normalized patterns were similar for EFI and ECAP, although the EFI patterns had much sharper peaks than the ECAP patterns (as quantified by the width of the pattern at 75 % of the peak amplitude). Note that the EFI pattern shapes may be affected by the estimation method for the electrical potentials on the stimulated electrodes. In contrast, the normalized PFM patterns had smaller areas under the curves than the normalized EFI and ECAP patterns, because the PFM patterns not only had sharp peaks but also kept decreasing toward both ends of the electrode array. For all three measurement methods, the normalized pattern areas were consistently smaller for $pTP_{(6,8,10)}$ than for $pTP_{(7,8,9)}$. A two-way RM ANOVA showed a significant effect of stimulation mode ($F_{1,\ 8} = 35.04$, $p = 0.004$), but not of measurement method ($F_{2,\ 8} = 0.80$, $p = 0.48$) or their interaction ($F_{2,\ 8} = 0.52$, $p = 0.61$), on the normalized pattern areas. On average, symmetrically spanned $pTP_{(6,8,10)}$ reduced the normalized pattern areas by 14 % as compared to standard $pTP_{(7,8,9)}$.

Correlation Between Pitch-Ranking Performance and Pattern Area Reduction

Among the features extracted from the normalized EFI, ECAP, and PFM patterns, only the areas under the curves significantly changed (more specifically, reduced) with symmetric spanning in pTP mode. Pearson correlation analyses were conducted to test whether the percentage reduction of the normalized pattern area may account for the inter-subject variability in pitch-ranking performance with symmetric spanning. The analyses showed no significant correlations between the percentage that $pTP_{(6,8,10)}$ was perceived as higher in pitch than $pTP_{(7,8,9)}$ (see Table 1) and the percentage reduction of the normalized pattern area with symmetric spanning ($r = -0.63$, $p = 0.25$ for EFI, $r = .10$, $p = 0.87$ for ECAP, and $r = -0.12$, $p = 0.85$ for PFM). Also note that the pitch-ranking performance with symmetric spanning was not correlated with the compensation coefficient of pTP stimuli, the age at testing, or the duration of CI use.

DISCUSSION

This study compared the EFI, ECAP, and PFM patterns of standard $pTP_{(7,8,9)}$ and symmetrically spanned $pTP_{(6,8,10)}$ to explain the higher pitch of $pTP_{(6,8,10)}$ than that of $pTP_{(7,8,9)}$. For each stimulus, the normalized EFI, ECAP, and PFM patterns differed from each other in shape details but had similar peaks, centroids, and areas under the curves. For the normalized EFI and PFM patterns, $pTP_{(6,8,10)}$ significantly reduced the pattern areas but did not shift the pattern peaks and centroids, as compared to $pTP_{(7,8,9)}$. These results suggest that the pitch increase

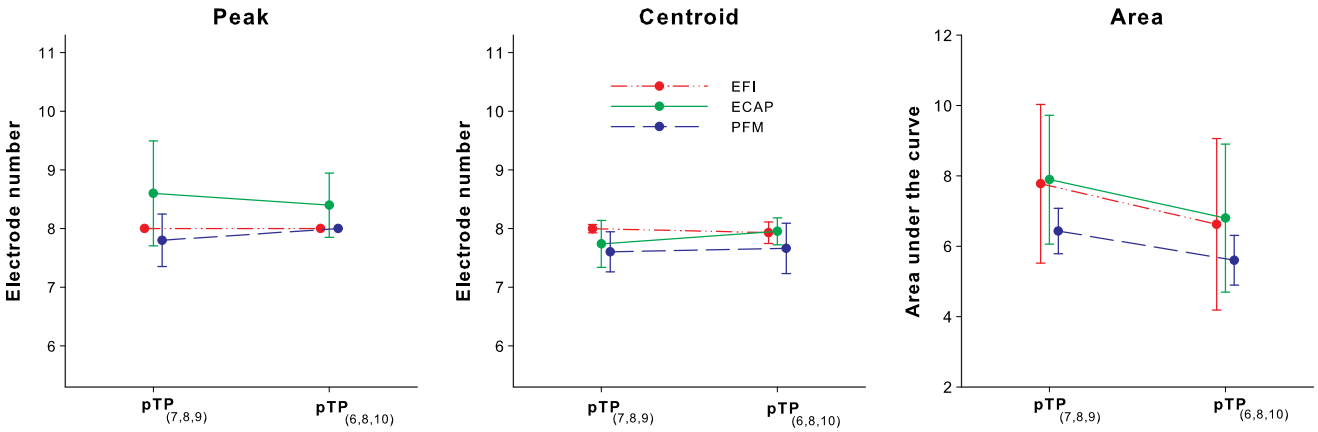

FIG. 4. Peaks (*left panel*), centroids (*middle panel*), and areas under the curves (*right panel*) of the normalized *EFI*, *ECAP*, and *PFM* patterns (*red*, *green*, and *blue circles*, respectively) for $pTP_{(7,8,9)}$ and $pTP_{(6,8,10)}$.

caused by symmetric spanning in pTP mode was likely due to an overall more focused excitation pattern rather than a basally shifted excitation peak or centroid. The pitch-ranking performance with symmetric spanning in pTP mode was not correlated with the percentage reduction of the normalized pattern area across subjects.

The present results were similar in many aspects to those of Wu and Luo (2016), because the same measurements were made in the same subjects for different stimuli. The measured patterns in both studies did not show any strong side lobes near the return electrodes or secondary excitation peaks away from the main electrode that may broaden the excitation patterns (e.g., Litvak et al. 2007). With the relatively small compensation coefficients, electrode spanning in this study did not increase the possibility of generating salient side lobes. Also, in both studies, there were no signs of dead regions near the main electrode EL8 (e.g., split or shifted peaks of excitation patterns or higher standard pTP-mode thresholds than those of the nearby main electrodes; see Bierer 2007).

The differences in shape details between the EFI, ECAP, and PFM patterns were partially due to the different stimulation parameters. For example, the areas around the peaks of the ECAP patterns were much broader than those of the EFI and PFM patterns, most likely because the ECAP patterns were measured with smaller compensation coefficients than the EFI and PFM patterns (see Table 1). As explained in the "Methods" section, smaller compensation coefficients were used to obtain reliable neural responses while sacrificing the degree of current focusing. The adopted stimulation parameters for ECAP recording worked well for all subjects except S3. In S3L and S3R, zero responses and non-monotonic changes happened in the ECAP patterns, respectively (but not in the EFI and PFM patterns). This showed the challenge of measuring ECAP responses to focused pTP stimuli, which only excited a small number of neurons (Zhu et al. 2012).

The different shape details of the EFI, ECAP, and PFM patterns also reflected the different processing at different stages along the auditory pathway. For example, the EFI patterns had a single sharp peak on EL8 and shallow tails on EL1–6 and EL10–16, while the PFM patterns (measured with the same compensation coefficients as the EFI patterns) showed a continuous roll-off from EL8 all the way to both ends of the electrode array. Wu and Luo (2016) pointed out that the amount of PFM on an electrode may rely on the masker electrical potentials and neural responses both on and off the electrode (see also Dingemanse et al. 2006). The PFM patterns may not just be a weighted integration of the EFI patterns, because the EFI estimated the voltage spread near the electrodes but not at the neural level. The different processing led to not only different shapes but also different effects of symmetric spanning for the EFI and PFM patterns. Despite possible estimation errors, the electrical potentials on EL7 and EL9 increased with symmetric spanning, similar to the modeling results of Wu and Luo (2014). However, the amounts of PFM on EL7 and EL9 decreased with symmetric spanning, suggesting that subjects may make use of the increased off-electrode listening for the probes, due to the reduced electrical potentials of the masker $pTP_{(6,8,10)}$ on EL1–6 and EL10–16.

The pitch increase caused by symmetric spanning in pTP mode may not have the same mechanism based on the excitation centroid as the pitch changes caused by current steering in pTP mode (Wu and Luo 2013, 2016). When symmetric spanning was applied to pTP stimuli, the measured EFI, ECAP, and PFM patterns showed generally symmetric reductions on both sides of the main electrode. This led to the unshifted pattern peaks and centroids, which cannot

explain the pitch increase caused by symmetric spanning. However, the possibility that such pitch increase is due to the shift of excitation peak or centroid cannot be completely excluded because the methods in this study had limitations. For example, the electrical potentials in the EFI on the stimulated electrodes could not be directly measured and had to be estimated. The ECAP responses could only be recorded for the pTP stimuli with shorter phase durations, lower pulse rates, smaller compensation coefficients, and lower loudness levels than those in the pitch-ranking test. Pitch increase with symmetric spanning was not verified for the ECAP stimuli, and the ECAP responses cannot be used to explain the pitch-ranking results of Wu and Luo (2014). Future studies should either develop methods to reliably record ECAP responses for the pitch-ranking stimuli in Wu and Luo (2014) or investigate the effect of symmetric spanning on pitch perception and PFM patterns for the ECAP stimuli in this study. For the PFM patterns, the probe threshold shifts were measured in decibel without taking into account the different dynamic ranges across the probe electrodes. The decibel values may be converted to the percentage of dynamic range in adjustment for perceptual relevance (McKay 2012). Also, the patterns may be normalized in other ways (e.g., linearly shifted to align the peaks or linearly scaled between the minimum and maximum values), which may alter the pattern shapes. However, there is no consensus on what the best normalization method should be.

The present results favored the hypothesis of Wu and Luo (2014) that symmetric spanning in pTP mode increased the perceived pitch by narrowing the excitation pattern. As mentioned in the "Introduction" section, this is likely a consequence of the interaction between timbre and pitch (e.g., Allen and Oxenham 2014; von Bismarck 1974). An overall more focused excitation pattern with symmetric spanning in pTP mode may generate a purer, cleaner sound quality with a greater pitch strength (e.g., Landsberger et al. 2012), which may be labeled as a pitch increase by subjects (e.g., Litvak et al. 2007). Symmetrically spanned $pTP_{(6,8,10)}$ produced narrower overall excitation patterns than $pTP_{(7,8,9)}$. This was more noticeable in the skirts of the excitation patterns and was because the non-adjacent return electrodes attenuated the electrical field of the main electrode more effectively than the adjacent return electrodes. Near the peaks, instead, the EFI patterns of $pTP_{(6,8,10)}$ appeared broader than those of $pTP_{(7,8,9)}$. In PFM measurement, the masker $pTP_{(7,8,9)}$ may be perceptually more similar to the standard pTP-mode probes than the masker $pTP_{(6,8,10)}$. The confusion effects between masker and probe (Cosentino et al. 2015; McKay 2012) may make $pTP_{(7,8,9)}$ a more effective masker with broader PFM patterns than $pTP_{(6,8,10)}$.

There is another possible explanation for the pitch increase caused by symmetric spanning in pTP mode. In acoustic hearing, the amplitude envelope of basilar membrane vibration is steeper at the apical edge than at the basal edge. As such, one may speculate that the place pitch does not correspond to the centroid of the neural excitation pattern but rather to a point close to the apical edge. If this were the case in this study, narrowing the excitation pattern with symmetric spanning in pTP mode would move the apical edge in the basal direction, leading to a higher pitch percept. However, the excitation patterns of acoustic and electric hearing have important differences in that asymmetry was found in the excitation patterns of acoustic hearing, whereas the PFM patterns measured in this study showed no evidence of steeper apical or basal edges of excitation in CIs. Thus, the above explanation is unlikely to hold for CI users.

Although the pitch increase caused by symmetric spanning in pTP mode may be explained by the reduction of the pattern area, there was no correlation between the pitch-ranking performance and pattern area reduction across subjects. Both the performance of pitch ranking and the reduction in pattern area were not correlated with the compensation coefficient that varied across subjects. The lack of correlation may be due to the small number of subjects and their consistently high pitch-ranking performance with symmetric spanning (see Table 1). In addition to the electrical fields and excitation patterns of the stimuli, peripheral factors such as neural survival and central factors such as the listening experience and cue weighting may have contributed to the pitch-ranking performance.

An important discovery of this study was that symmetric spanning in pTP mode can narrow the excitation pattern in CI users. The percentage reduction of the pattern area from standard pTP mode to symmetrically spanned pTP mode in this study was on average similar to that from MP mode to standard pTP mode in Landsberger et al. (2012). Because speech perception in noise has been shown to significantly improve with focused standard pTP mode than with MP mode (Srinivasan et al. 2013), similar improvements in speech perception in noise may be expected with symmetrically spanned pTP mode than with standard pTP mode. Also, when the same compensation coefficient was used, standard and symmetrically spanned pTP modes required similar current levels to reach the most comfortable level. Therefore, symmetric spanning in pTP mode has the potential to further increase frequency selectivity and reduce channel interaction for CI

users. Of course, the improved spectral resolution with symmetrically spanned pTP mode has yet to be shown in clinical settings with multiple electrodes turned on. It is also unclear how speech perception may be affected by the possible changes in sound quality with spanned pTP mode (e.g., increase in pureness/cleanness that may be confused as increase in pitch). Future studies may use symmetrically spanned pTP mode for all channels in a CI speech processing strategy, except the two lowest and highest channels that do not have a non-adjacent apical and basal return electrode, respectively.

This study and Wu and Luo's (2014) only tested spanned pTP mode in which return electrodes were spaced one electrode away from the main electrode. A question worth asking is whether return electrodes spaced two or more electrodes away from the main electrode are more effective in reducing the current spread. Note that the excitation peak and centroid are expected to remain around the main electrode as long as the electrode spanning is symmetric. The electrode spacing that generates the most focused excitation pattern may rely on the compensation coefficient, because for a certain electrode spacing, a high compensation coefficient may increase the salience of the side lobes to broaden instead of narrowing the excitation pattern. The interaction between electrode spacing and compensation coefficient for excitation pattern and pitch perception should be tested in the future. It is also interesting to quantify the pitch increase with symmetric spanning in pTP mode. For example, the pitch of the symmetrically spanned pTP stimulus may be compared to those of the standard pTP stimuli on nearby main electrodes to measure the pitch increase with symmetric spanning in terms of electrodes. In CI users with single-sided deafness, acoustic stimuli presented to the non-implanted ear may be pitch-matched to the standard and symmetrically spanned pTP stimuli (e.g., Carlyon et al. 2010). In this way, the pitch increase with symmetric spanning in pTP mode can be measured in Hz.

ACKNOWLEDGMENTS

We are grateful to all subjects for their participation in the experiments. Research was supported in part by NIH (R21-DC-011844).

COMPLIANCE WITH ETHICAL STANDARDS

All subjects gave informed consent and were compensated for their participation. This study was approved by the Purdue IRB committee.

REFERENCES

ABBAS PJ, BROWN CJ, SHALLOP JK, FIRSZT JB, HUGHES ML, HONG SH, STALLER SJ (1999) Summary of results using the nucleus CI24M implant to record the electrically evoked compound action potential. Ear Hear 20(1):45–59

ALLEN EJ, OXENHAM AJ (2014) Symmetric interactions and interference between pitch and timbre. J Acoust Soc Am 135(3):1371–9

BERENSTEIN CK, VANPOUCKE FJ, MULDER JJS, MENS LHM (2010) Electrical field imaging as a means to predict the loudness of monopolar and tripolar stimuli in cochlear implant patients. Hear Res 270(1-2):28–38

BIERER JA (2007) Threshold and channel interaction in cochlear implant users: evaluation of the tripolar electrode configuration. J Acoust Soc Am 121(3):1642–1653

BIERER JA (2010) Probing the electrode-neuron interface with focused cochlear implant stimulation. Trends Amplif 14(2):84–95

BIERER JA, BIERER SM, MIDDLEBROOKS JC (2010) Partial tripolar cochlear implant stimulation: spread of excitation and forward masking in the inferior colliculus. Hear Res 270(1-2):134–142

CARLYON RP, MACHEREY O, FRIJNS JHM, AXON PR, KALKMAN RK, BOYLE P, DAUMAN R (2010) Pitch comparisons between electrical stimulation of a cochlear implant and acoustic stimuli presented to a normal-hearing contralateral ear. J Assoc Res Otolaryngol 11(4):625–640

COSENTINO S, DEEKS JM, CARLYON RP (2015) Procedural factors that affect psychophysical measures of spatial selectivity in cochlear implant users. Trends Hear 19:1–16

DINGEMANSE JG, FRIJNS JHM, BRIAIRE JJ (2006) Psychophysical assessment of spatial spread of excitation in electrical hearing with single and dual electrode contact maskers. Ear Hear 27(6):645–657

GOLDWYN JH, BIERER SM, BIERER JA (2010) Modeling the electrode-neuron interface of cochlear implants: effects of neural survival, electrode placement, and the partial tripolar configuration. Hear Res 268(1-2):93–104

JOLLY CN, SPELMAN FA, CLOPTON BM (1996) Quadrupolar stimulation for cochlear prostheses: modeling and experimental data. IEEE Trans Biomed Eng 43(8):857–865

LANDSBERGER DM, PADILLA M, SRINIVASAN AG (2012) Reducing current spread using current focusing in cochlear implant users. Hear Res 284(1-2):16–24

LITVAK LM, SPAHR AJ, EMADI G (2007) Loudness growth observed under partially tripolar stimulation: model and data from cochlear implant listeners. J Acoust Soc Am 122(2):967–981

MCKAY CM (2012) Forward masking as a method of measuring place specificity of neural excitation in cochlear implants: a review of methods and interpretation. J Acoust Soc Am 131(3):2209–24

MENS LHM, BERENSTEIN CK (2005) Speech perception with mono- and quadrupolar electrode configurations: a crossover study. Otol Neurotol 26(5):957–964

MIDDLEBROOKS JC, SNYDER RL (2007) Auditory prosthesis with a penetrating nerve array. J Assoc Res Otolaryngol 8(2):258–279

SRINIVASAN AG, PADILLA M, SHANNON RV, LANDSBERGER DM (2013) Improving speech perception in noise with current focusing in cochlear implant users. Hear Res 299:29–36

TYKOCINSKI M, SAUNDERS E, COHEN LT, TREABA C, BRIGGS RJS, GIBSON P, COWAN RSC (2001) The contour electrode array: safety study and initial patient trials of a new perimodiolar design. Otol Neurotol 22(1):33–41

VANPOUCKE FJ, ZAROWSKI AJ, PEETERS SA (2004A) Identification of the impedance model of an implanted cochlear prosthesis from intracochlear potential measurements. IEEE Trans Biomed Eng, 51(12): 2174–2183

Vanpoucke F, Zarowski A, Casselman J, Frijns J, Peeters S (2004b) The facial nerve canal: an important cochlear conduction path revealed by Clarion electrical field imaging. Otol Neurotol, 25(3): 282–289

von Bismarck G (1974) Sharpness as an attribute of the timbre of steady sounds. Acustica 30:159–172

Wu CC, Luo X (2013) Current steering with partial tripolar stimulation mode in cochlear implants. J Assoc Res Otolaryngol 14(2):213–231

Wu C-C, Luo X (2014) Electrode spanning with partial tripolar stimulation mode in cochlear implants. J Assoc Res Otolaryngol 15(6):1023–1036

Wu C-C, Luo X (2016) Excitation patterns of standard and steered partial tripolar stimuli in cochlear implants. J Assoc Res Otolaryngol, http://doi.org/10.1007/s10162-015-0549-1

Zhu Z, Tang Q, Zeng FG, Guan T, Ye D (2012) Cochlear-implant spatial selectivity with monopolar, bipolar and tripolar stimulation. Hear Res 283(1-2):45–58